I&EC research
Industrial & Engineering Chemistry Research
pubs.acs.org/IECR
Article

Assessment of Structural and Separation Properties of a PVDF/PD Composite Membrane Incorporated with TiO_2 Nanotubes and SiO_2 Particles

Mehrnaz Safarnia, Majid Pakizeh,* and Mahdieh Namvar-Mahboub

Cite This: *Ind. Eng. Chem. Res.* 2021, 60, 659−669
Read Online

ABSTRACT: The current study focuses on the preparation of a polydopamine (PD)-modified PVDF membrane and its application for drug removal. The effect of adding an inorganic compound (TEOS) on the characteristics and performance of the PD/PVDF thin-film composite (TFC) membrane has also been investigated. For this purpose, the PD layer was coated using TEOS for in situ synthesis of a silica layer. The resultant membrane was coated at different dosages of as-synthesized TNTs to prepare thin-film nanocomposite membranes (TFN(S-T)). The prepared TNT, TFC, and TFN membranes were characterized by employing transmission electron microscopy (TEM), attenuated total reflection Fourier transform infrared (ATR-IR) spectroscopy, field emission scanning electron microscopy (FESEM), energy-dispersive X-ray (EDX), atomic force microscopy (AFM), ζ potential, and contact angle measurements. The results confirmed the formation of a hydrophilic nanocomposite layer with a negative charge. The separation performance of the as-prepared membranes was evaluated via diclofenac removal. The results revealed that diclofenac rejection increased from 81.5% for the PVDF membrane to 91.6% for the PD/silica/PVDF membrane with a permeability of 2.5 L/(m^2·h·bar). In the case of the TFN(S-T) membrane, drug rejection increased to 93.2% at 0.1% TNTs and the permeability improved to 5.8 L/(m^2·h·bar). Also, the effects of pH and feed concentration on diclofenac separation performance were studied. The results implied that the rejection of diclofenac increased from 93.2 to 95.6% with an increase in pH from 7 to 10.

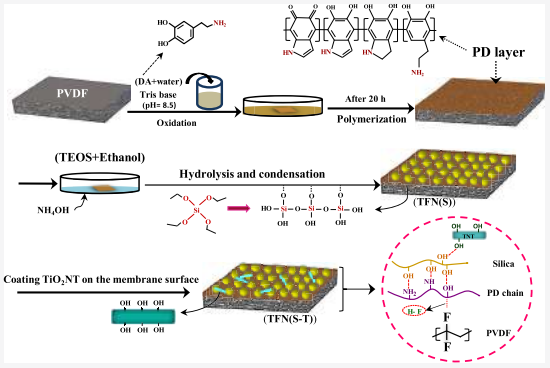

1. INTRODUCTION

Pharmaceutical compounds enter the environment through the production process or domestic effluents.[1] These contaminants cause health, environmental, and economic concerns due to their unwanted effect on the aquatic system.[2,3] It is worth noting that the consumption, toxicity, and persistence of drugs such as beta blockers, anti-inflammatory drugs, and steroid hormones used for cancer treatment and antibiotics are considered environmentally important.[4] Among all, diclofenac, being a highly toxic, nonsteroidal, and anti-inflammatory drug, has been considered one of the most widely introduced pharmaceutical pollutants into the environment. It has varying toxic effects on several aquatic organisms such as Daphnia magna, trout, embryos, and larvae.[2] Due to its hazardous effects, the elimination of diclofenac from wastewater is of primary concern.

Cost and energy-efficiency as well as environmentally friendly purification technologies are the subjects of new research being conducted on treating water. Different techniques like adsorption, oxidation, membrane processes, and membrane bioreactors (MBRs) are applied to remove pharmaceutical compounds from wastewater.[5] Membrane techniques are particularly favored over other water treatment techniques due to their distinct advantages resulting in better water quality, nonuse of chemical additives, and excellent separation efficiency. High-pressure membrane techniques, including nanofiltration (NF) and reverse osmosis (RO), are considered promising technologies in the removal of trace pharmaceutical compounds with high reliability and stability.[6,7] A literature review shows that there have so far been few studies on diclofenac removal from aqueous solutions. For instance, Vergili[8] studied the performance of the commercial NF membrane for the separation of carbamazepine, diclofenac, and ibuprofen. He reported that a maximum rejection of 88% with a water permeance of 7 L/(m^2·h·bar) was obtained for diclofenac using an FMNP010 membrane. Ge et al.[9] applied an NF270 commercial membrane to remove 14 kinds of drugs from water. They achieved a maximum rejection of 85% with a water

Received: December 8, 2020
Accepted: December 11, 2020
Published: December 29, 2020

https://dx.doi.org/10.1021/acs.iecr.0c06045
Ind. Eng. Chem. Res. 2021, 60, 659−669

permeance of 10.5 L/(m^2·h·bar) for diclofenac. Wang et al.[10] studied the performance of a TFN zeolite nanofiltration membrane for the removal of diclofenac. They reported a rejection of 92% and a permeance of 2 L/(m^2·h·bar). Maryam et al.[11] investigated the performance of an NF50 commercial membrane via drug separation. They used dead-end filtration module to remove 99.74% of diclofenac from water while the permeability was very low. In all of the mentioned cases, commercial membranes were thin-film composite or polymeric membranes.

Over the past decades, polymers have remained the most widely used materials for the preparation of water treatment membranes because of their good separation performance.[2] Among the different polymers, poly(vinylidene fluoride) (PVDF) has become a much-coveted research topic in the membrane industry due to its excellent chemical resistance and thermal stability.[12] However, low surface energy and strong hydrophobic properties of the PVDF membrane limit its practical application in wastewater treatment.[13,14] Polymeric membranes are usually used in the development of a thin, dense active layer on the top of a porous substrate.[15] Among the various available compounds, polydopamine (PD) has been demonstrated as a promising material due to its compact structure and strong adhesion property on a wide range of substrates that find applications in various fields.[16] Additionally, hydrophilic nanomaterials can be used in the form of nanotubes, nanosheets, or nanoparticles to improve the surface properties and morphology of the resultant membranes. In this case, the resultant nanocomposite membranes can be formed via solution blending or in situ synthesis of a hybrid inorganic−polymer nanocomposite. Besides, nanomaterials are most probably coated or covalently bonded on the membrane surface to improve hydrophilicity, surface charge density, and antifouling property of membranes.[15] For instance, Xu et al. applied a graphene oxide-TiO_2 nanocomposite to improve the photodegradation efficiency of the PVDF UF membrane.[17] Ma et al. reported the positive effect of oxidized multiwall carbon nanotubes (MWCNTs) on the performance of the PVDF UF membrane.[18] They proved that the oxygen-containing groups of MWCNTs played a key role in improving the structural properties and the performance of the resultant membranes. Other nanomaterials such as TiO_2, Al_2O_3, SiO_2, and Fe_3O_4 are a proper group of inorganic fillers that can be used for the modification of membranes. Pertaining to the additives mentioned above, TiO_2 is considered an appropriate modifier because of its stability, commercial availability, ease of preparation, low cost, and super hydrophilic properties.[19,20] As reported in the literature, titania nanotubes (TNTs) demonstrate high specific surface area and pore volumes, which provide abundant adsorption sites and diffusion channels for water molecules.[21] Accordingly, direct water passage can be provided by TNTs, leading to improved water permeability. Additionally, as it is known, well-dispersed nanoparticles such as silica can be formed on membrane surfaces via in situ synthesis techniques. Tetraethoxysilane (TEOS) is the most common source of silica, which is applied to prepare silica−polymer matrices via hydrolysis and condensation processes.[22] As reported by Zhao et al.,[23] the silica−polydopamine hybrids were appropriately formed on the surface of the polypropylene support membrane.

Based on investigations that have been conducted and the observations that have been made to date, there are no reports that have considered the effect of both thin-film coating and nanomaterials simultaneously on the performance of the PVDF membrane for drug removal.

Accordingly, the current work aimed at the preparation of a surface-modified PD/PVDF thin-film membrane using silica and as-synthesized TNTs as additives to improve the rejection and permeability. The effects of the TNT dosage on the surface chemistry and morphology of the resultant TFN membranes were investigated by ATIR-FTIR, FESEM, ζ potential, EDX, AFM, and contact angle analysis. Additionally, the potential application of the as-prepared membranes was evaluated for diclofenac removal from aqueous solutions. Finally, the effects of feed concentration and the solution pH on the separation performance of the prepared membranes were investigated.

2. EXPERIMENTAL SECTION

2.1. Materials. Poly(vinylidene fluoride) (MW = 440 000 g/mol, Kynar 761) was purchased from Arkema Co.; LiCl powder, *N*-methyl-2-pyrrolidone (NMP, ≥99%), TEOS, and *n*-hexane were obtained from Merck KGaA (Germany); dopamine hydrochloride, trimesoyl chloride (TMC), and Tris base were purchased from Sigma-Aldrich; and ammonium hydroxide was purchased from Fluka Co. (Switzerland). Titanium dioxide nanoparticles (TiO_2, Degussa P25, Evonik) were used to synthesize titania nanotubes (TNTs). Sodium hydroxide (NaOH, Merck) and hydrochloric acid (HCl, Merck) were also used to modify the TNTs. Diclofenac (MW = 369.3 g/mol, ≥99.9%) was supplied by Sobhan Pharmaceutical, Iran. Deionized (DI) water was used to prepare feed solutions and also to soak and rinse the membrane samples during the experiments.

2.2. Preparation of TNTs. TNTs were synthesized via the hydrothermal method.[24] For this, 0.5 g of commercial anatase TiO_2 powder was added to 50 mL of 10 M NaOH. The mixture was stirred at ambient temperature for 30 min. Then, the mixture was heated in a Teflon autoclave at 150 °C. A white product was centrifugally separated, washed with 1 M HCl and deionized water, and then dried at 80 °C for 4 h. Finally, the as-synthesized TNTs were posttreated at 500 °C for 3 h.

2.3. Preparation of Membranes. *2.3.1. Support Membrane.* PVDF was dissolved in NMP to prepare a casting solution containing 14 wt % PVDF at 50 °C. A pore former was added into the solution with a LiCl/PVDF weight ratio of 0.1. Then, the solution was stirred for 4 h. The homogeneous solution was degassed for 24 h. The polymeric solution was cast on a clean glass plate using a casting knife (200 μm gap). The film was immediately immersed in a coagulation water bath for 24 h at 24 °C.

2.3.2. Preparation of the PD/PVDF Membrane. A coating solution was prepared by mixing dopamine hydrochloride and a Tris base buffer solution (pH = 8.5). The PVDF support membrane was immersed in the dopamine solution for 20 h to ensure self-polymerization of dopamine. Then, PD was cross-linked with TMC (0.4 wt %) through interfacial polymerization for 2 min. Then, the composite membrane was dried in an oven at 40 °C for 30 min.

2.3.3. Preparation of the Silica/PD/PVDF Membrane. First, the PVDF membrane was immersed in a dopamine solution (pH = 8.5) for 20 h and was thoroughly rinsed with deionized water and dried in an oven (50 °C) to get the PD-PVDF film. A TEOS solution was prepared by dissolving 0.3 g of tetraethylorthosilicate in water/ethanol/ammonium hydroxide (3:40:1 mL). The PD/PVDF membrane was placed in the TEOS solution

https://dx.doi.org/10.1021/acs.iecr.0c06045
Ind. Eng. Chem. Res. 2021, 60, 659−669

under stirring for 24 h and was then dried in a vacuum oven (50 °C) for 30 min.

2.3.4. Preparation of the TNTs/Silica/PD/PVDF Membrane. TNTs were incorporated on the surface of the PD/silica layer via two distinct methods. In the first method, a certain amount of the as-synthesized TNTs (0.05, 0.1, 0.3%) was dispersed in deionized water via 1 h sonication. Then, the PD/silica/PVDF membrane was placed in contact with TNT suspensions for 1 h to form TFN membranes including both silica and TNTs nanofillers (TFN(S-T)). The as-prepared membranes were named based on the TNT concentrations.

In the second method, 0.1% TNT was added to the TEOS solution to prepare the TEOS-TNT dispersion. The resultant membrane was named TFN(S-T)-0.1(b) to differ from TFN(S-T). The membrane at the same TNT concentration via the first method was named TFN(S-T)-0.1(a). Other steps of preparation were conducted exactly similar to the one in the PD/silica/PVDF preparation method. Table 1 shows the codes of the as-prepared membranes.

Table 1. Code of TFC and TFN As-Prepared Membranes

code	membrane
PVDF	support membrane
TFC	PVDF/PD membrane
TFN(S)	PVDF/PD/silica membrane
TFN(S-T)-0.05	PVDF/PD/silica/TNT (0.05%) membrane
TFN(S-T)-0.1(a)	PVDF/PD/silica/TNT (0.1%) membrane
TFN(S-T)-0.3	PVDF/PD/silica/TNT (0.3%) membrane
TFN(S-T)-0.1(b)	PVDF/PD/silica + TNT membrane (0.1 wt % in layer matrix)

2.4. Membrane Characterizations. Transmission electron microscopy (TEM) analysis was performed to study the morphological structure of the produced TNTs (LEO 912 AB, Germany). The topography of the surface and cross-sections of the as-prepared membrane samples were observed using a field emission scanning electron microscope (FESEM; Tescan; Czech Republic). The functional groups and bonds of the TFC and TFN membranes were analyzed using attenuated total reflectance infrared (ATR-IR) spectroscopy. ATR-FTIR was applied using a Thermo Nicolet Nexus 100 ATR-IR coupled to a ZnSe crystal at a 45° operating angle. Atomic force microscopy (AFM) was used to analyze the surface morphology and roughness of the prepared membranes. The AFM device was an Easyscan 2 Flex instrument (Nanosurf AG, Switzerland). For comparative analysis, the scan area was kept constant at 5 × 5 μm^2 for all of the samples. The sessile drop contact angle method of DI water and an OCA15 plus goniometer (DataPhysics Instruments USA Corp.) were used to measure the membrane contact angles of samples. The data of water contact angles were reported as the average of measurements obtained from at least five water droplets on each membrane surface. The ζ potential of the surface of composite membranes was measured at neutral pH by employing a streaming potential analyzer (Anton Paar; Austria) in a 0.001 mol/L KCl aqueous solution at 25 °C.

2.5. Membrane Performance. The performance of the as-prepared membranes was investigated by the diclofenac removal from aqueous solutions. Experiments were carried out at a diclofenac concentration of 50 mg/L using the cross-flow permeation test as shown in Figure 1 with an effective membrane

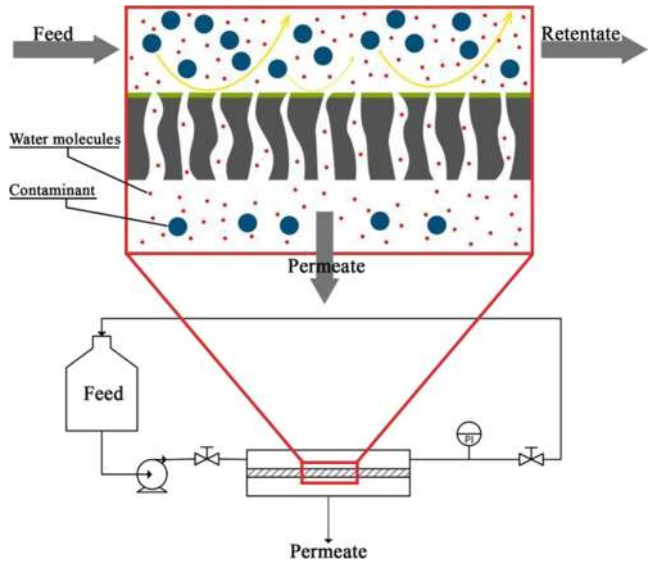

Figure 1. Schematic of the cross-flow recirculation membrane filtration setup.

area of 0.0096 m^2. All permeation tests were conducted at a constant temperature of 25 °C and a pressure of 7.0 bar. Performance parameters were evaluated in terms of PWF (pure water flux) and diclofenac rejection. All membranes were pressured at 8.0 bar with DI water for at least 1.5 h to reach a stable PWF before each test.

The flux and permeability (L/(m^2·h·bar)) were calculated as follows

$$J = \frac{V}{A \cdot \Delta t} \tag{1}$$

$$p = \frac{J}{\Delta P} \tag{2}$$

where V is the permeate volume (L), A is the effective permeation area of the membrane (m^2), Δt is the collection time of the permeate (h), and P is the pressure (bar).

The solute rejection (R) is calculated as follows

$$R = \left(1 - \frac{C_P}{C_F}\right) \times 100 \tag{3}$$

where C_P and C_F are the solute concentrations in the permeate and feed streams, respectively. For all experiments, the permeate flux and rejection were determined after 1.5 h. All of the experiments were performed at least three times. The ultraviolet−visible (UV−vis) concentration of different diclofenac solutions was measured with an ultraviolet spectrophotometer (Optizen POP; Mecasys; South Korea) at 276 nm.

3. RESULTS AND DISCUSSION

3.1. Morphology of TNTs. Figure 2 illustrates the TEM and FESEM images of as-synthesized TNTs, showing the nanotubular structure with an average inner diameter of about 14 nm. It was observed that the TNTs are in the shape of cylindrical tubes. Nanotubes were obtained by the heat treatment of crystalline titania nanoparticles in NaOH solution followed by washing of the suspension by DI water and dilute hydrochloric acid solution.[24] The mechanism of TNT formation was explained by Kasuga et al.[25] as follows. During the synthesis procedure, some Ti−O−Ti bonds of titania nanoparticles were

https://dx.doi.org/10.1021/acs.iecr.0c06045
Ind. Eng. Chem. Res. 2021, 60, 659−669

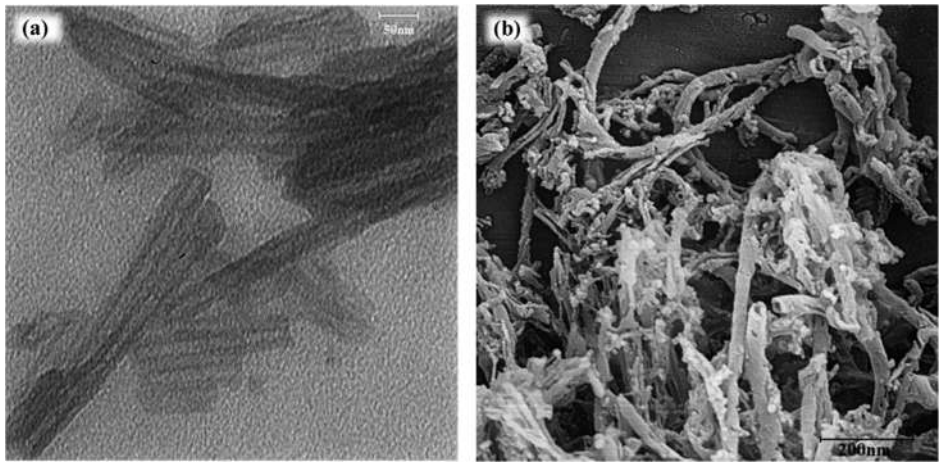

Figure 2. (a) TEM and (b) FESEM images of TiO_2 nanotubes.

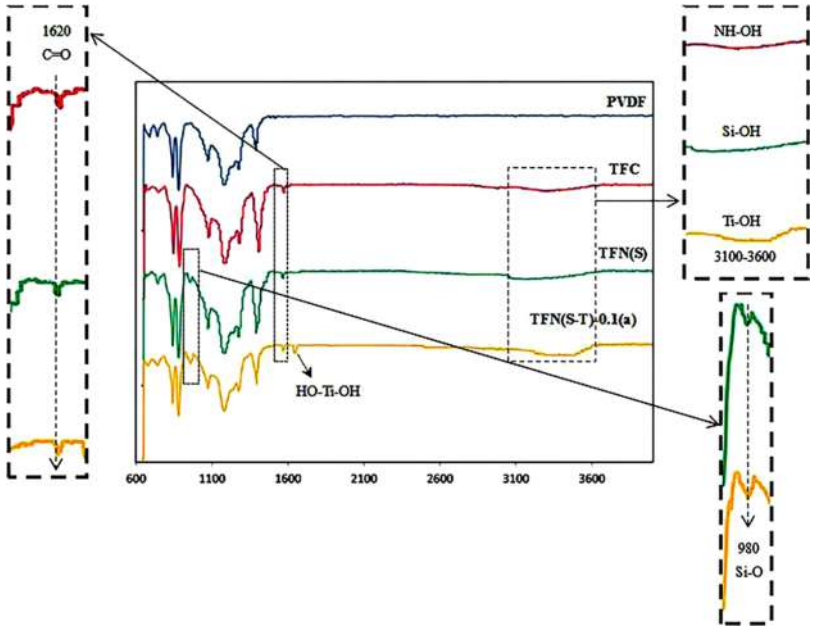

Figure 3. ATR-IR spectra for the surfaces of TFN, TFC, and support membranes.

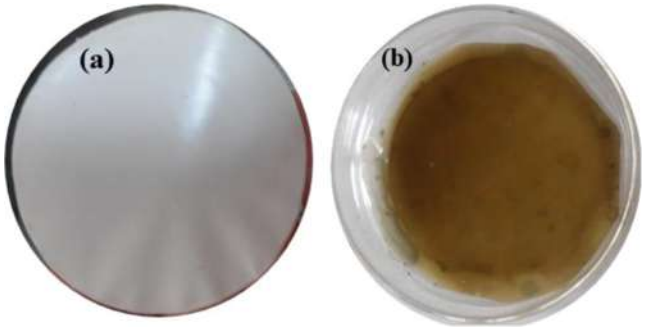

Figure 4. (a) PVDF surface and (b) PVDF/PD surface.

broken; subsequently, Ti−O−Na bonds were formed in the presence of the NaOH solution. These bonds were substituted by TiOH bonds after washing with water. Finally, TiOH of the resultant nanosheet was dehydrated to form Ti−O−Ti or Ti−HO−Ti bonds, owing to treatment with dilute HCl solution. This led to bond distance shrinkage and felting of nanosheets.

3.2. ATR-FTIR Spectra of the As-Prepared Membranes.

The surface properties of the as-prepared membranes were studied using ATR-FTIR analysis. The ATR-FTIR spectra of neat and modified PVDF membranes are shown in Figure 3. For the PVDF membrane, the peak at 1180 cm^{-1} was associated with CF_2. The peak at 1280 cm^{-1} was assigned to the vibration of the C−F bond.[26] The absorption peak appearing at 1400 cm^{-1} was attributed to the CH wagging vibration.[27] The peaks at 880 and 740 cm^{-1} were assigned to the C−C−C asymmetrical stretching vibration and the vibration of the crystalline phase of PVDF, respectively.[26] After PD coating, the support membrane became dark brown, indicating that the PD layer was deposited on the PVDF membrane surface (Figure 4b).[27] This finding was further confirmed via ATR-FTIR spectra. As can be seen, in the case of TFC, new peaks were observed at 3100−3600 cm^{-1} related to N−H/O−H stretching and 1620 cm^{-1} corresponding to C═O stretching in the benzene aromatic ring. These peaks confirmed the presence of catecholamine and quinone in the PD layer.[14] For the TFN(S) membrane, the peak at 980 cm^{-1} was assigned to the Si−O stretching of the Si−O−Si of the silica chain.[28] In

https://dx.doi.org/10.1021/acs.iecr.0c06045
Ind. Eng. Chem. Res. 2021, 60, 659−669

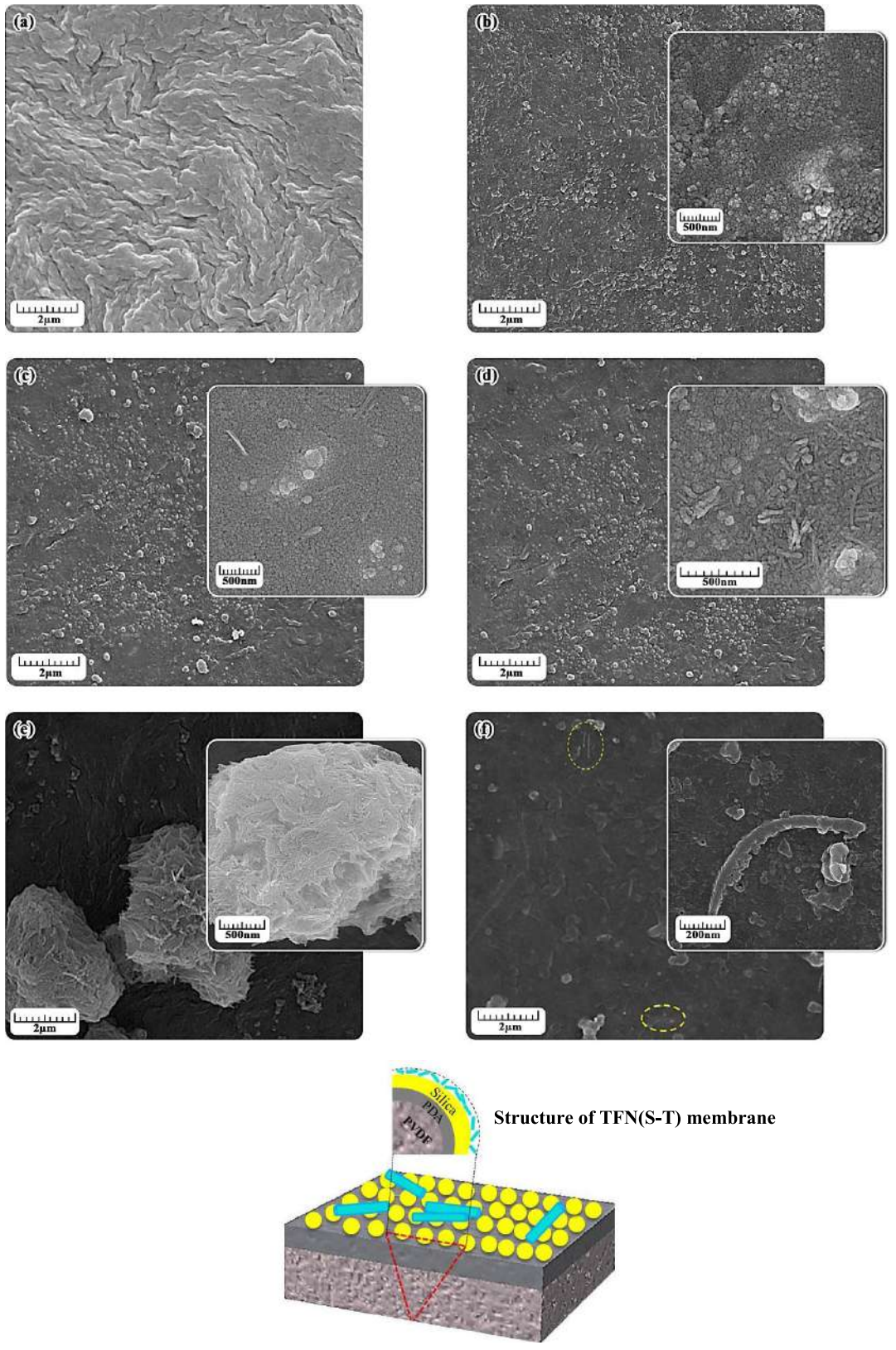

Figure 5. FESEM surface images of (a) PVDF, (b) TFN(S), (c) TFN(S-T)-0.05, (d) TFN(S-T)-0.1(a), (e) TFN(S-T)-0.3, and (f) TFN(S-T)-0.1(b).

the case of the TFN(S-T) membrane, increasing peak intensity between 3200 and 3500 cm^{-1} was attributed to the stretching vibrations of the hydroxyl groups of TNTs.[21] These active groups formed hydrogen-bonding interactions with Si−OH on the silica so that the composite coating was firmly fixed to the surface of the membrane. The band at 1649 cm^{-1} was attributed to the H−O−H binding vibration due to the presence of nanotubes.[29,30]

https://dx.doi.org/10.1021/acs.iecr.0c06045
Ind. Eng. Chem. Res. 2021, 60, 659−669

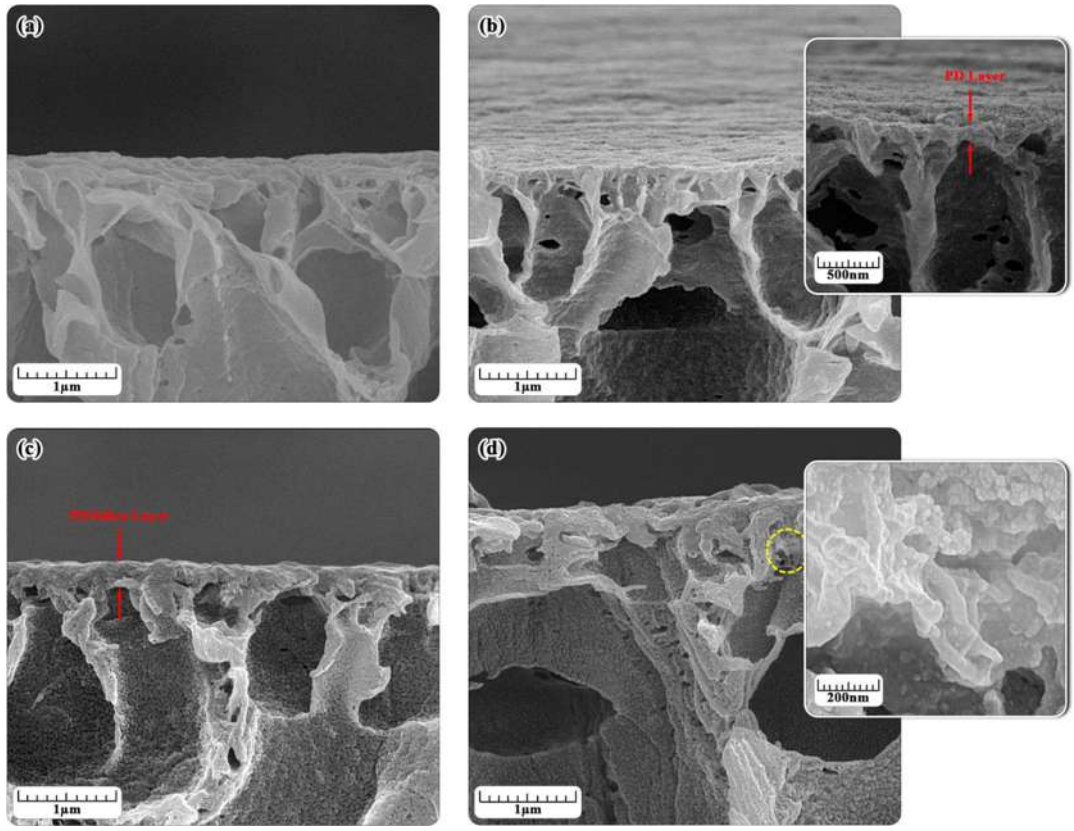

Figure 6. Cross-sectional images of the prepared membranes: (a) PVDF, (b) TFC, (c) TFN(S), and (d) TFN(S-T)-0.1(b).

3.3. Membrane Morphology. FESEM analysis was used to investigate the effect of PD coating, silica, and TNTs on the morphology of the as-prepared membranes.

Figure 5 shows the surface images of the samples. As can be seen in Figure 5b, for the TFN(S) membrane, the surface morphology has noticeably changed due to the formation of the PD/silica layer, which was confirmed by the ATR-FTIR results. A similar PD structure has been reported in other studies.[14,31] TEOS was hydrolyzed and condensed during the coating procedure; as a result, SiO_2 nanoparticles were formed over the PVDF/PD membrane.[23] In the case of the TFN(S-T) membrane, some TNTs can be observed at a high magnification of FESEM surface images. At a low dosage of 0.05 and 0.1% TNTs, nanotubes were well deposited on the surface of the PD/silica/PVDF membrane (Figure 5c,d). As can be seen clearly from Figure 5e, by increasing the TNT dosage from 0.1 to 0.3%, nanotubes aggregated on the surface of the resultant membrane.

The cross-sectional images of the support membrane, TFC, TFN(S), and (TFN(S-T)-0.1(b)) are presented in Figure 6.

As can be seen, for the TFC membrane, the PD thin layer was formed on the surface of the PVDF membrane after the coating process (Figure 6b). In the case of the PVDF/PD/silica membrane, the PD/silica selective layer was uniformly formed on the top surface of the PVDF membrane (Figure 6c). It is to be noted that in situ synthesized silica nanoparticles have interacted with the PD chain during the coating process. For the TFN(S-T)-0.1(b) membrane, Figure 6d shows the presence of TNTs in the layer matrix. TNTs interacted with silica and the PD layer, simultaneously.

EDX analysis was performed to confirm the concept of silica formation in the top layer matrix of the PVDF/PD/silica membrane. Additionally, the presence of TNTs on the structure of the TFN(S-T)-0.1(b) membrane was confirmed by the EDX spectra. Figure 7 presents the EDX spectra of both TFN(S) and TFN(S-T)-0.1(b) membranes. As can be observed, for both cases, the characteristic peaks of C and F are those belonging to the PVDF support. Additionally, the peaks of N and Si elements confirm the formation of silica and the PD layer. In Figure 7b, the peaks of the Ti element confirm the dispersion of TNTs in the selective layer of TFN(S-T)-0.1(b).

3.4. Surface Roughness, Charge, and Hydrophilicity of the As-Prepared Membranes. The three-dimensional AFM images of the as-prepared membranes are illustrated in Figure 8. The surface roughness parameters of the abovementioned membranes were also evaluated, and the average values of three replicates are reported in Table 2. As shown, the PVDF membrane accounts for the lowest roughness value of 3.09 nm and increased to 4.75 nm for TFN(S). The results indicated that the surface roughness of the PVDF membrane increased after coating with the PD/silica layer. This can be attributed to the formation of PD and silica particles, which imposed inhomogeneous deposition on the membrane surface.[32] By incorporation of TNTs (0.05%), R_a remained approximately unchanged. However, by increasing the TNT dosage, at 0.1%, the surface roughness increased to a higher value due to the presence of TNTs for both TNF(S-T)-0.1(a) and TNF(S-T)-0.1-(b).[19,33−35] For TFN(S-T)-0.3, the roughness increased significantly to 14.36 nm due to the agglomeration of nanotubes on the surface.

The surface hydrophilicity of the as-prepared membranes was evaluated by measuring the water contact angle, and the average values are shown in Figure 9a. As illustrated, the contact angle for the PVDF membrane was 87°. After surface modification of PVDF with the PD/silica layer, the contact angle decreased to

https://dx.doi.org/10.1021/acs.iecr.0c06045
Ind. Eng. Chem. Res. 2021, 60, 659−669

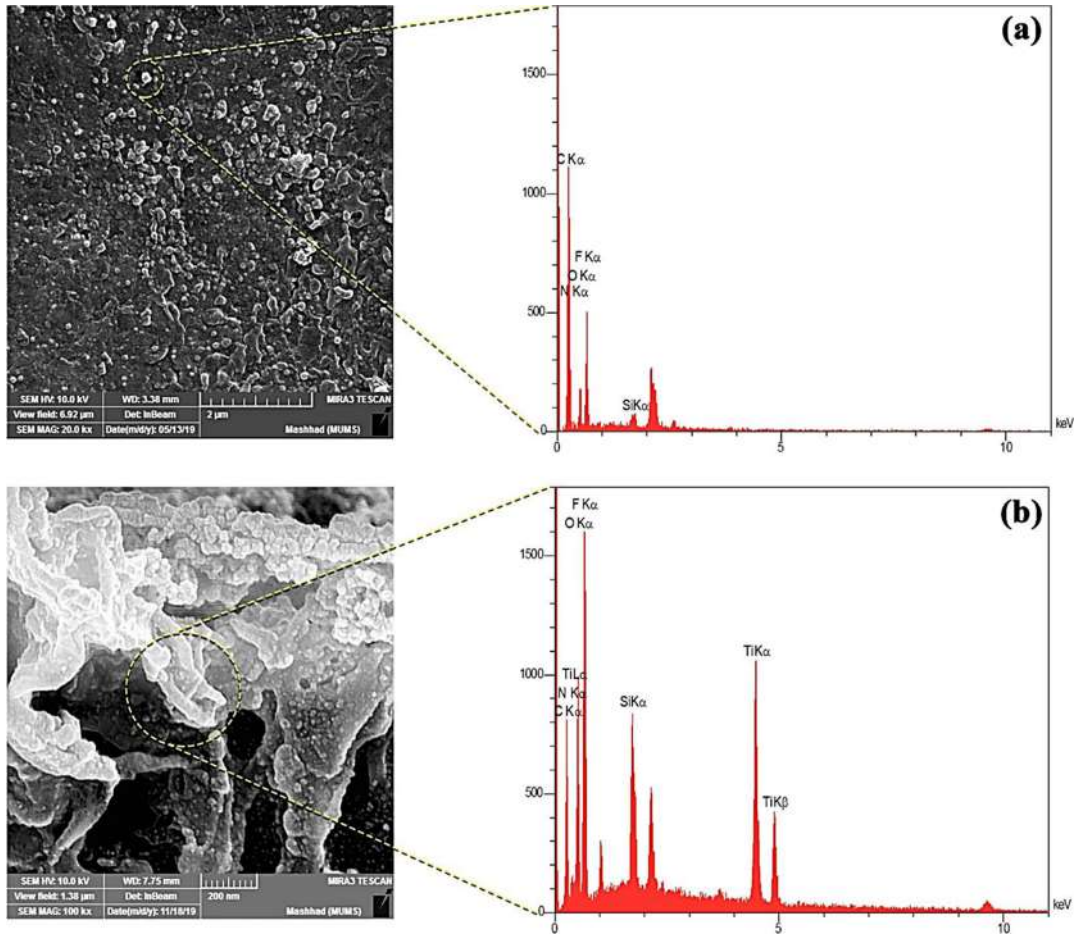

Figure 7. EDX analysis of (a) TFN(S) and (b) (TFN(S-T)-0.1(b)).

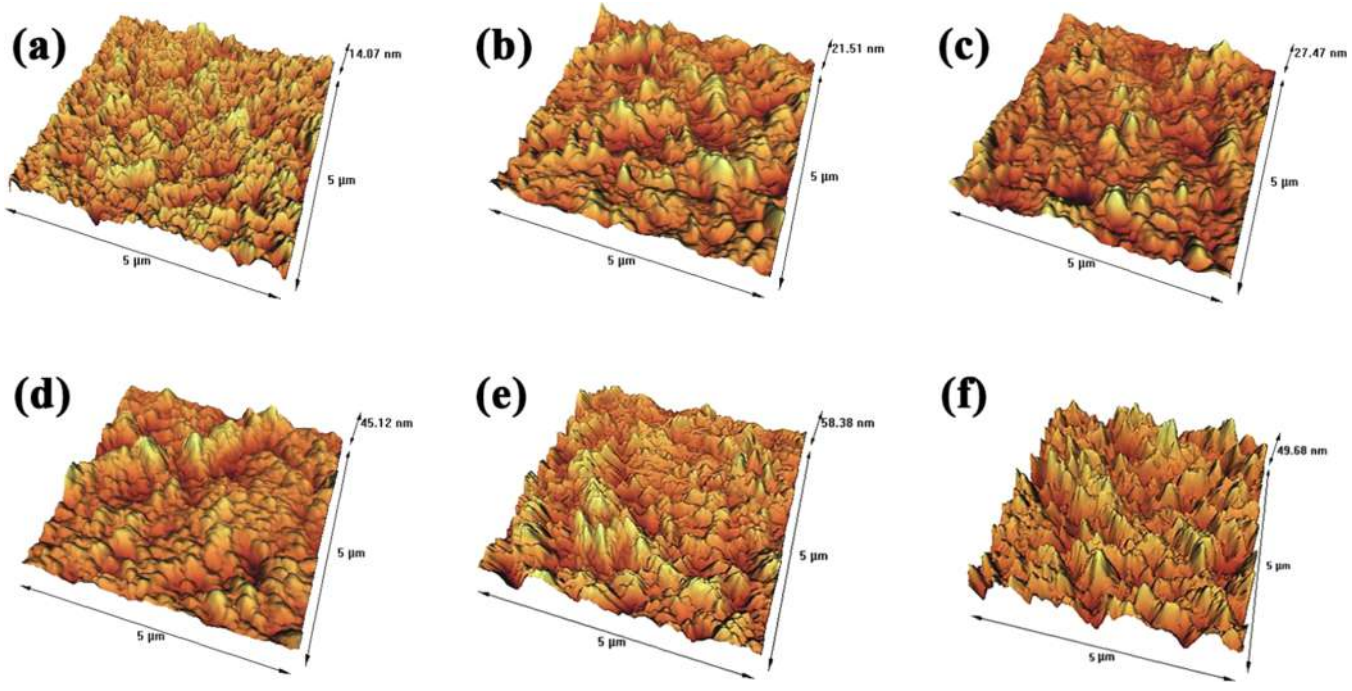

Figure 8. AFM images of (a) PVDF, (b) TFN(S), (c) TFN(S-T)-0.05, (d) TFN(S-T)-0.1(a), (e) TFN(S-T)-0.3, and (f) TFN-0.1(b).

69°. When 0.05 and 0.1% of TNTs were deposited on the PD/silica/PVDF membrane surface, the contact angle decreased to 60 and 44°, respectively. This trend could be due to the presence of hydroxyl groups of TNTs on the top surface of the resultant

https://dx.doi.org/10.1021/acs.iecr.0c06045
Ind. Eng. Chem. Res. 2021, 60, 659−669

Table 2. Surface Roughness Parameters of the As-Prepared Membranes

membrane	R_q (nm)	R_a (nm)
PVDF	3.91 ± 0.03	3.094 ± 0.59
TFN(S)	5.97 ± 0.93	4.71 ± 0.56
TFN(S-T)-0.05	6.23 ± 0.95	5.04 ± 0.51
TFN(S-T)-0.1(a)	10.87 ± 1.14	8.75 ± 0.87
TFN(S-T)-0.3	17.58 ± 1.01	14.36 ± 0.83
TFN(S-T)-0.1(b)	19.69 ± 1.47	17.95 ± 1.04

TFN(S-T) membrane.[19,36] By increasing the TNT dosage from 0.1 to 0.3%, no obvious reduction in the contact angle was observed due to the agglomeration of TNTs.

The electrical charge of the PVDF and TFN(S-T) membranes was also determined by the ζ potential analysis (Figure 9b). As indicated, the surface of the TFN(S-T)-0.1(a) membrane became more negatively charged. The absolute value of the surface ζ potential at a pH of 7.0 increased from 14.7 mV for the PVDF membrane to 21 mV for TFN(S-T). This was attributed to the presence of hydroxyl groups related to TNTs and the PD/silica layer.[37]

3.5. Separation Performance. The performance parameters including permeability and drug rejection of pure PVDF, TFC, and TFN membranes are shown in Figure 10. For pure PVDF, a permeability of 9.5 L/(m^2·h·bar) and a rejection of 81.5% were obtained. By dopamine coating on the PVDF surface (TFC), the permeability decreased to 2.5 L/(m^2·h·bar) and the rejection increased to 87%. Also, for the TFN(S) membrane, diclofenac rejection increased to 91.6% with a permeability of 2.6 L/(m^2·h·bar). According to the FESEM and contact angle results, the hydrophilicity of the PD/silica/PVDF membrane increased due to the presence of amine and hydroxyl functional groups, while the surface pore size decreased. In the case of the TFN(S) membrane, it seems that the effect of the membrane morphology has overcome the surface hydrophilicity; as a consequence, permeability has decreased.[38] Actually, the improvement in diclofenac rejection was due to the formation of the PD and SiO_2 protective layer.[23]

Figure 10 shows that the deposition of TNTs on the TFN(S) membrane has slightly improved the rejection of diclofenac. By increasing the TNT dosage from 0 to 0.1%, the solute rejection increased from 91.6 to 93.2%, which was the maximum rejection

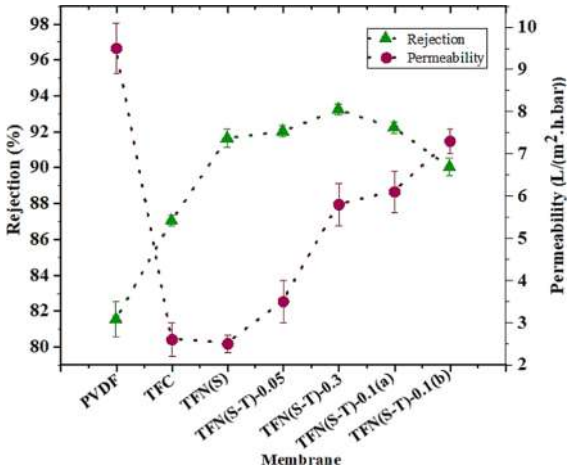

Figure 10. Performance of the as-prepared membranes through diclofenac removal (pH = 7, T = 24 °C, and ΔP = 7 bar).

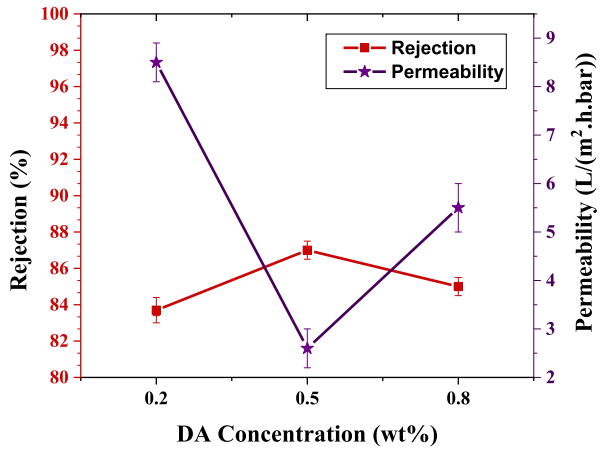

Figure 11. Effect of dopamine concentration (pH = 7, T = 24 °C, and ΔP = 7 bar).

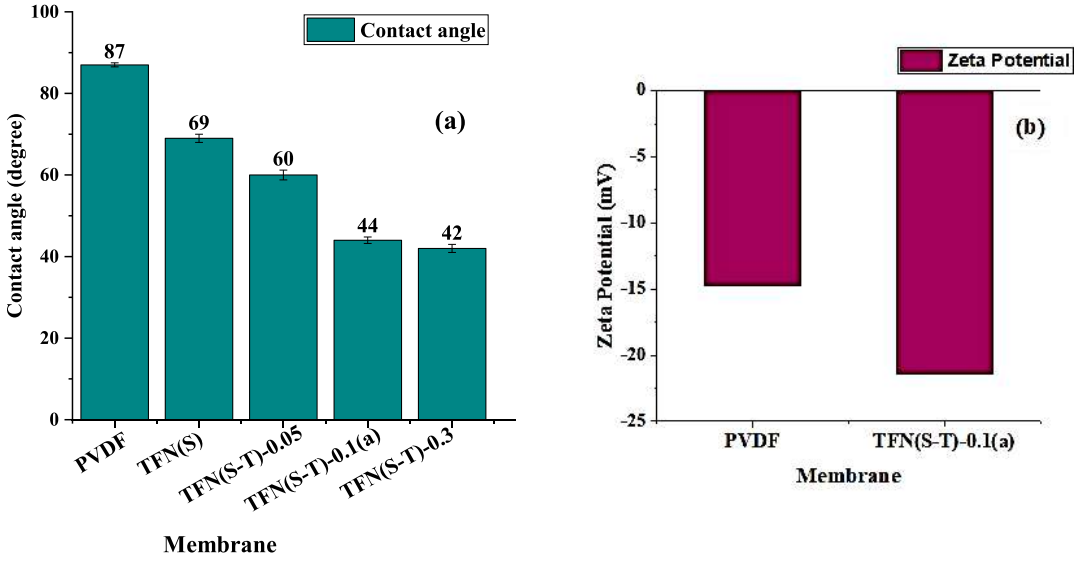

Figure 9. (a) Contact angle of the as-prepared membranes and (b) ζ potential of the membranes.

https://dx.doi.org/10.1021/acs.iecr.0c06045
Ind. Eng. Chem. Res. 2021, 60, 659−669

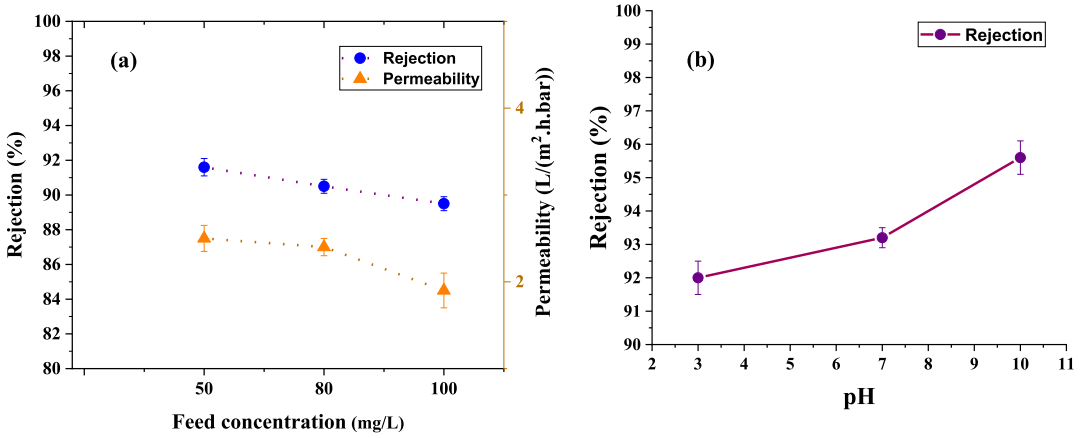

Figure 12. Effect of (a) feed concentration on the TFN(S) membrane (pH = 7) and (b) solution pH on the TFN(S-T)-0.1(a) membrane.

value. In addition, permeability increased from 2.5 to 5.8 L/(m^2·h·bar). These trends can be explained according to the following mechanisms.

Diclofenac may be rejected by the as-prepared membranes through one or a combination of three mechanisms: (i) molecular sieving, (ii) electrostatic repulsion, and (iii) adsorption. The presence of the hydroxyl groups of TNTs increases the surface hydrophilicity, thereby enhancing the transportation of water molecules through the membrane.[39] Additionally, TNTs plug the surface pores, resisting the passage of diclofenac through the membrane and thus decreasing the diclofenac rejection.[19] Moreover, diclofenac with a dissociation constant of 4.15 has a negative charge at pH = 7. The ζ potential results (Figure 9b) depict that TFN(S-T)-0.1(a) is more negatively charged than the PVDF membrane. In this case, more solute removal has been detected due to electrostatic repulsion.[40] However, by increasing the TNT dosage to 0.3%, the nanotubes were agglomerated and heterogeneously distributed on the membrane surface. Accordingly, the TNTs plugging the pores and the negative charge on the TFN membrane surface reduced, leading to the lower solute rejection of TFN(S-T)-0.3 compared with that of TFN(S-T)-0.1(a).

For the TFN(S-T)-0.1(b) membrane, a solute rejection of 90% and a permeability of 7.3 L/(m^2·h·bar) were observed. The results revealed that the formation of the silica-TNT composite improved the water flux. Both the tubular structure and hydroxyl functional groups of TNTs played a critical role in increasing the water transportation rate.[41] Since the water molecules are about the size of an Angstrom, they can easily pass through the structure of the nanotubes. Indeed, the inner cores of the nanotubes and the less compact in situ synthesized silica-TNT layer created an additional passage for the transportation of the solvent or diclofenac molecules.[41] Additionally, the octanol–water partition coefficient (K_{ow}) of pharmaceuticals can be applied as an important factor to explain the separation mechanism. As known, molecules with log K_{ow} > 2 are hydrophobic.[8,42] Since the log K_{ow} of diclofenac is 4.51, it can be considered as a moderate hydrophobic material. Therefore, by improving the surface hydrophilicity of the membrane, more diclofenac molecules may be rejected due to their hydrophobic nature.

3.6. Effect of Different Factors on Membrane Performance. *3.6.1. Effect of Dopamine Concentration.* To investigate the effect of the concentration on the performance of the selective layer of the TFC membrane, different concentrations of dopamine (0.2, 0.5, and 0.8%) were used to form the PD layer. Figure 11 represents the rejection and permeability values of the resultant TFC membrane. As can be seen, by increasing the dopamine concentration, the permeability first decreased and then increased. However, diclofenac rejection depicted an inverse trend, and at 0.5 wt % dopamine, a drug rejection of 87% and a permeability of 2.5 L/(m^2·h·bar) were obtained. Lee et al.[14] reported that at a low concentration of dopamine, a loose layer was formed, and by increasing its concentration, a denser layer was obtained. Indeed, the low density of the PD layer was related to poor cross-linking at low dopamine concentrations.[43] On the other hand, at high dopamine concentrations, the TMC-to-dopamine ratio decreased and excess dopamine particles caused defects in the PD layer.[14]

3.6.2. Effect of Feed Concentration. The effect of feed concentration (50, 80, and 100 mg/L) and an operating pressure of 7 bar on the performance of the TFN(S) membrane was investigated. Figure 12a showed that by increasing the feed concentration from 50 to 100 mg/L, both permeability and drug rejection were decreased, which can be explained via fouling formation.[44] As it is known, the increase of feed concentration results in concentration polarization and consequently more surface fouling.[19]

3.6.3. Effect of pH on Separation. In general, the solution pH affects the charge of most organic contaminants. Thus, the effect of the solution pH (3, 7, and 10) on the TFN(S-T)-0.1(a) membrane performance was investigated (Figure 12b). As can be observed, the drug rejection increased from 92% at pH = 3 to 95.6% at pH = 10. Regarding the dissociation constant of diclofenac (pK_a = 4.15), solute molecules have a positive charge at pH = 3 and a negative charge at pH = 7 and 10. Moreover, the as-prepared TFN membrane depicted a negative charge due to the presence of hydroxyl groups. Accordingly, it can be stated that electrostatic interaction and repulsion play a critical role in the separation mechanism.

At pH values less than pK_a, positively charged diclofenac molecules tend to adsorb on the surface of the membrane due to electrostatic interactions. By increasing the solution pH from 3 to 7, the solute attained a negative charge, which led to electrostatic interaction between the solute and the surface of the membrane. At higher pH values (≥10), the strong electrostatic repulsion between the functional groups caused membrane swelling and pore shrinkage of the selective layer.[37]

https://dx.doi.org/10.1021/acs.iecr.0c06045
Ind. Eng. Chem. Res. 2021, 60, 659−669

4. CONCLUSIONS

In this work, the characteristics and performance of the PD/silica/TNT/PVDF membrane were investigated. For this purpose, the TEOS solution was coated on the PD layer where silica was synthesized via the hydrolysis and condensation of TEOS. FESEM and EDX analyses confirmed the formation of the PD nanocomposite layer. Additionally, the TEOS-modified PD layer was coated at different dosages of as-synthesized TNTs to prepare the TFN(S-T) membrane. For comparison, the optimum dosage of TNTs was added to the TEOS coating solution. The as-synthesized TNT, TFC, and TFN membranes were characterized and the obtained results confirmed the formation of a negatively charged nanocomposite layer. Moreover, the surface hydrophilicity of the PVDF membrane significantly increased in the presence of PD and inorganic additives. The performance of the as-prepared membranes was determined for diclofenac removal. The results revealed that the diclofenac rejection of the PVDF membrane increased by about 14% through the PD/silica/TNT modification of PVDF. Also, the effects of pH and feed concentration on the diclofenac separation performance were studied. The results indicated that the rejection of diclofenac increased from 93.2 to 95.6% with an increase of pH from 7 to 10.

AUTHOR INFORMATION

Corresponding Author

Majid Pakizeh − *Department of Chemical Engineering, Faculty of Engineering, Ferdowsi University of Mashhad, 9177948974 Mashhad, Iran; Department of Chemical Engineering, Hamedan University of Technology, 6516913733 Hamedan, Iran*; Email: pakizeh@hut.ac.ir

Authors

Mehrnaz Safarnia − *Department of Chemical Engineering, Faculty of Engineering, Ferdowsi University of Mashhad, 9177948974 Mashhad, Iran*; orcid.org/0000-0002-1287-4632

Mahdieh Namvar-Mahboub − *Department of Chemical Engineering, University of Gonabad, 9691957678 Gonabad, Iran*

Complete contact information is available at: https://pubs.acs.org/10.1021/acs.iecr.0c06045

Notes

The authors declare no competing financial interest.

ACKNOWLEDGMENTS

The authors acknowledged the assistance of Ferdowsi University of Mashhad Central Laboratory and Ferdowsi University of Mashhad Separation Processes Laboratory.

REFERENCES

(1) Topal, M.; Arslan Topal, E. I. Optimization of tetracycline removal with chitosan obtained from mussel shells using RSM. *J. Ind. Eng. Chem.* **2020**, *84*, 315−321.

(2) Nadour, M.; Boukraa, F.; Benaboura, A. Removal of Diclofenac, Paracetamol and Metronidazole using a carbon-polymeric membrane. *J. Environ. Chem. Eng.* **2019**, *7*, No. 103080.

(3) Leal, J. E.; Thompson, A. N.; Brzezinski, W. A. Pharmaceuticals in drinking water: Local analysis of the problem and finding a solution through awareness. *J. Am. Pharm. Assoc.* **2010**, *50*, 600−603.

(4) Salomão, G. R.; Américo-Pinheiro, J. H. P.; Isique, W. D.; Torres, N. H.; Cruz, I. A.; Ferreira, L. F. R. Diclofenac removal in water supply by adsorption on composite low-cost material. *Environ. Technol.* **2019**, 1−17.

(5) Chtourou, M. Pharmaceutical and Personal Care Products Removal by Advanced Treatment Technologies. Ph.D. Dissertation, University of Girona: Spain, 2018.

(6) Liu, Y. L.; Wang, Xm.; Yang, Hw.; F. Xie, Y. Quantifying the influence of solute-membrane interactions on adsorption and rejection of pharmaceuticals by NF/RO membranes. *J. Membr. Sci.* **2018**, *551*, 37−46.

(7) Sri Abirami Saraswathi, M. S.; Rana, D.; Divya, K.; Alwarappan, S.; Nagendran, A. Fabrication of anti-fouling PVDF nanocomposite membranes using manganese dioxide nanospheres with tailored morphology, hydrophilicity and permeation. *New J. Chem.* **2018**, *42*, 15803−15810.

(8) Vergili, I. Application of nanofiltration for the removal of carbamazepine, diclofenac and ibuprofen from drinking water sources. *J. Environ. Manage.* **2013**, *127*, 177−187.

(9) Ge, S.; Feng, L.; Zhang, L.; Xu, Q.; Yang, Y.; Wang, Z.; Kim, K. Rejection rate and mechanisms of drugs in drinking water by nanofiltration technology. *Environ. Eng. Res.* **2017**, *22*, 329−338.

(10) Dong, L. X.; Huang, X. C.; Wang, Z.; Yang, Z.; Wang, X. M.; Tang, C. Y. A thin-film nanocomposite nanofiltration membrane prepared on a support with in situ embedded zeolite nanoparticles. *Sep. Purif. Technol.* **2016**, *166*, 230−239.

(11) Maryam, B.; Buscio, V.; Odabasi, S. U.; Buyukgungor, H. A study on behavior, interaction and rejection of Paracetamol, Diclofenac and Ibuprofen (PhACs) from wastewater by nanofiltration membranes. *Environ. Technol. Innov.* **2020**, *18*, No. 100641.

(12) Rahimpour, A.; Madaeni, S. S.; Zereshki, S.; Mansourpanah, Y. Preparation and characterization of modified nano-porous PVDF membrane with high antifouling property using UV photo-grafting. *Appl. Surf. Sci.* **2009**, *255*, 7455−7461.

(13) Wang, H.; Gong, R.; Qian, X. Preparation and Characterization of TiO_2/g-C_3N_4/PVDF Composite Membrane with Enhanced Physical Properties. *Membranes* **2018**, *8*, 14.

(14) Ji, Y.-L.; Belle, M.; Yap, M.; Hung, H.; Huang, S.; Quan-Fu, A.; Lee, K.; Lai, J. Bio-inspired deposition of polydopamine on PVDF followed by interfacial cross-linking with trimesoyl chloride as means of preparing composite membranes for isopropanol dehydration. *J. Membr. Sci.* **2018**, *557*, 58−66.

(15) Akther, N.; Phuntsho, S.; Chen, Y.; Ghaffour, N.; Kyong, H. Recent advances in nanomaterial-modified polyamide thin-film composite membranes for forward osmosis processes. *J. Membr. Sci.* **2019**, *584*, 20−45.

(16) Saraswathi, M. S. S. A.; Rana, D.; Alwarappan, S.; Gowrishankar, S.; Vijayakumar, P.; Nagendran, A. Polydopamine layered poly (ether imide) ultrafiltration membranes tailored with silver nanoparticles designed for better permeability, selectivity and antifouling. *J. Ind. Eng. Chem.* **2019**, *76*, 141−149.

(17) Xu, Z.; Wu, T.; Shi, J.; Teng, K.; Wang, W.; Ma, M.; Li, J.; Qian, X.; Li, C.; Fan, J. Photocatalytic antifouling PVDF ultrafiltration membranes based on synergy of graphene oxide and TiO_2 for water treatment. *J. Membr. Sci.* **2016**, *520*, 281−293.

(18) Ma, J.; Zhao, Y.; Xu, Z.; Min, C.; Zhou, B.; Li, Y.; Li, B.; Niu, J. Role of oxygen-containing groups on MWCNTs in enhanced separation and permeability performance for PVDF hybrid ultrafiltration membranes. *Desalination* **2013**, *320*, 1−9.

(19) Cheshomi, N.; Pakizeh, M.; Namvar-Mahboub, M. Preparation and characterization of TiO_2/Pebax/(PSf-PES) thin film nanocomposite membrane for humic acid removal from water. *Polym. Adv. Technol.* **2018**, *29*, 1303−1312.

(20) Shaban, M.; AbdAllah, H.; Said, L.; Hamdy, H.; Khalek, A. A. Titanium dioxide nanotubes embedded mixed matrix PES membranes characterization and membrane. *Chem. Eng. Res. Des.* **2015**, *95*, 307−316.

(21) Emadzadeh, D.; Lau, W. J.; Rahbari-sisakht, M.; Ilbeygi, H.; Rana, D.; Matsuura, T.; Ismail, A. F. Synthesis, modification and optimization of titanate nanotubes- polyamide thin film nanocomposite

(TFN) membrane for forward osmosis (FO) application. *Chem. Eng. J.* **2015**, *281*, 243−251.
(22) Wang, Z. X.; Jiang, X.; Cheng, X. Q.; Lau, C. H.; Shao, L. Mussel-Inspired Hybrid Coatings that Transform Membrane Hydrophobicity into High Hydrophilicity and Underwater Superoleophobicity for Oil-in-Water Emulsion Separation. *ACS Appl. Mater. Interfaces.* **2015**, *7*, 9534−9545.
(23) Zhao, Y.; Si, L.; Dang, W.; Lu, Z. Facile construction of silica-based surface coating onto polypropylene microporous film through dopamine-assisted hydrolysis of tetraethoxysilane. *Ceram. Int.* **2018**, *44*, 10192−10198.
(24) Roy, P.; Berger, S.; Schmuki, P. TiO_2 Nanotubes: Synthesis and Applications. *Angew. Chem., Int. Ed.* **2011**, *50*, 2904−2939.
(25) Kasuga, B. T.; Hiramatsu, M.; Hoson, A.; Sekino, T.; Niihara, K. Titania Nanotubes Prepared by Chemical Processing. *Adv. Mater.* **1999**, *567*, 1307−1311.
(26) Wang, J.; Zheng, L.; Wu, Z.; Zhang, Y.; Zhang, X. Fabrication of hydrophobic flat sheet and hollow fiber membranes from PVDF and PVDF-CTFE for membrane distillation. *J. Membr. Sci.* **2016**, *497*, 183−193.
(27) Saraswathi, M. S. A.; Kausalya, R.; Kaleekkal, N. J.; Rana, D.; Nagendran, A. BSA and humic acid separation from aqueous stream using polydopamine coated PVDF ultrafiltration membranes. *J. Environ. Chem. Eng.* **2017**, *5*, 2937−2943.
(28) Kunst, S. R.; Cardoso, H. R. P.; Oliveira, C. T.; Santana, J. A.; Sarmento, V. H. V.; Muller, I. L.; Malfatti, C. F. Corrosion resistance of siloxane-poly(methyl methacrylate) hybrid films modified with acetic acid on tin plate substrates: Influence of tetraethoxysilane addition. *Appl. Surf. Sci.* **2014**, *298*, 1−11.
(29) López de Dicastillo, C.; Patiño, C.; Galotto, M. J.; Palma, J. L.; Alburquenque, D.; Escrig, J. Novel Antimicrobial Titanium Dioxide Nanotubes Obtained through a Combination of Atomic Layer Deposition and Electrospinning Technologies. *J. Nanomater.* **2018**, *8*, 128.
(30) Jasmeen, N. Synthesis of Titanium Oxide Nanotube via Hydrothermal Method and Recovery of Palladium by means of it. *Open J. Nano* **2013**, *2*, 2−5.
(31) Jiang, J.; Zhu, L.; Zhu, L.; Baoku, Z.; Youyi, X. Surface characteristics of a self-polymerized dopamine coating deposited on hydrophobic polymer films. *Langmuir* **2011**, *27*, 14180−14187.
(32) Xi, Z.; Xu, Y.; Zhu, L.; Wang, Y.; Zhu, B. A facile method of surface modification for hydrophobic polymer membranes based on the adhesive behavior of poly(DOPA) and poly(dopamine). *J. Membr. Sci.* **2009**, *327*, 244−253.
(33) Li, J.; Ni, X.; Zhang, D.; Zheng, H.; Wang, J.; Zhang, Q. Engineering a self-driven PVDF/PDA hybrid membranes based on membrane micro-reactor effect to achieve super-hydrophilicity, excellent antifouling properties and hemocompatibility. *Appl. Surf. Sci.* **2018**, *444*, 672−690.
(34) Zuo, J.; Cheng, P.; Chen, X.; Yan, X.; Guo, Y.; Lang, W. Ultrahigh flux of polydopamine-coated PVDF membranes quenched in air via thermally induced phase separation for oil /water emulsion separation. *Sep. Purif. Technol.* **2018**, *192*, 348−359.
(35) Xiang, Y.; Liu, F.; Xue, L. Under seawater superoleophobic PVDF membrane inspired by polydopamine for efficient oil/seawater separation. *J. Membr. Sci.* **2015**, *476*, 321−329.
(36) Vatanpour, V.; Ghadimi, A.; Karimi, A.; Khataee, A.; Yekavalangi, M. E. Antifouling polyvinylidene fluoride ultrafiltration membrane fabricated from embedding polypyrrole coated multiwalled carbon nanotubes. *Mater. Sci. Eng. C.* **2018**, *89*, 41−51.
(37) Medhat Bojnourd, F.; Pakizeh, M. Separation and Purification Technology Preparation and characterization of a PVA /PSf thin film composite membrane after incorporation of PSSMA into a selective layer and its application for pharmaceutical removal. *Sep. Purif. Technol.* **2018**, *192*, 5−14.
(38) Shi, H.; He, Y.; Pan, Y.; Di, H.; Zeng, G.; Zhang, L.; Zhang, C. A modified mussel-inspired method to fabricate TiO_2 decorated super-hydrophilic PVDF membrane for oil/water separation. *J. Membr. Sci.* **2016**, *506*, 60−70.
(39) Baroña, G. N. B.; Choi, M.; Jung, B. High permeate flux of PVA /PSf thin film composite nanofiltration membrane with aluminosilicate single-walled nanotubes. *J. Colloid Interface Sci.* **2012**, *386*, 189−197.
(40) Baroña, G. N. B.; Lim, J.; Choi, M.; Jung, B. Interfacial polymerization of polyamide-aluminosilicate SWNT nanocomposite membranes for reverse osmosis. *Desalination* **2013**, *325*, 138−147.
(41) Amini, M.; Jahanshahi, M.; Rahimpour, A. Synthesis of novel thin-film nanocomposite (TFN) forward osmosis membranes using functionalized multi-walled carbon nanotubes. *J. Membr. Sci.* **2013**, *435*, 233−241.
(42) Dias, S. F. L.; Nogueira, S. S.; de França Dourado, F.; Guimarães, M. A.; de Oliveira Pitombeira, N.A.; Gobbo, G. G.; Primo, F. L.; de Paula, R.C.M.; Feitosa, J. P. A.; Tedesco, A. C.; Nunes, L. C. C.; Leite, J. R. S. A.; da S ilva, D.A. Acetylated cashew gum-based nanoparticles for transdermal delivery of diclofenac diethyl amine. *Carbohydr. Polym.* **2016**, *143*, 254−261.
(43) Zhao, J.; Su, Y.; He, X.; Zhao, X.; Li, Y.; Zhang, R.; Jiang, Z. Dopamine composite nanofiltration membranes prepared by self-polymerization and interfacial polymerization. *J. Membr. Sci.* **2014**, *465*, 41−48.
(44) Ngang, H. P.; Ooi, B. S.; Ahmad, A. L.; Lai, S. O. Preparation of PVDF-TiO_2 mixed-matrix membrane and its evaluation on dye adsorption and UV-cleaning properties. *Chem. Eng. J.* **2012**, *197*, 359−367.

https://dx.doi.org/10.1021/acs.iecr.0c06045
Ind. Eng. Chem. Res. 2021, 60, 659−669